



# Reactivity of Sodium Pentaphospholide Na[*cyclo*-P<sub>5</sub>] towards C≡E (E = C, N, P) Triple Bonds

Andrey Petrov,<sup>[a]</sup> Lawrence Conrad,<sup>[b]</sup> Nathan T. Coles,<sup>[a, c]</sup> Manuela Weber,<sup>[a]</sup> Dirk Andrae,<sup>[b]</sup> Almaz Zagidullin,<sup>[d]</sup> Vasili Miluykov,<sup>[d]</sup> and Christian Müller\*<sup>[a]</sup>

**Abstract:** A diglyme solution of Na[*cyclo*-P<sub>5</sub>] (1) reacts with alkynes and isolobal nitriles and phosphalkynes to afford the otherwise elusive (aza)phospholide anions **2a–c**, **4a,b**, and **6**. The reaction of Na[*cyclo*-P<sub>5</sub>] with alkynes and nitriles was studied by means of DFT methods, which suggested a concerted mechanism for the formation of **2a** and **4b**. The

anions **2a–c**, **4a,b**, and **6** coordinate in an  $\eta^5$ -fashion towards Fe<sup>II</sup> to give the sandwich (aza)phosphametalloenes **3a–c**, **5a,b** and **7** in moderate to good yields. The new compounds were characterized by means of multinuclear NMR spectroscopy, single-crystal X-ray diffraction and cyclic voltammetry.

## Introduction

Hückel aromaticity usually refers to cyclic planar hydrocarbons with delocalized  $4n+2$   $\pi$ -electrons that feature increased thermodynamic stability. To date, a number of aromatic species containing main group elements have also been described. The replacement of CH fragments with heteroatoms leads to significant changes in the electronic properties of the corresponding compound and thus has been of great interest both for synthetic and theoretical chemists.<sup>[1]</sup> Special attention is given to aromatic five- and six-membered  $\lambda^3\sigma^2$  heterocycles with incorporated pnictogen elements in low coordination, such as nitrogen and phosphorus. In fact, the trivalent heteroatoms are isolobal to an  $sp^2$ -hybridized CH unit. Moreover, N/P-heterocycles possess energetically low-lying LUMOs that can assist in the stabilization of electron-rich metal centers through  $\eta^5$  or  $\eta^6$  coordination. Additionally, the accessible lone

pairs of the heteroelements expand the scope of binding modes that are impossible for classical cyclic hydrocarbons.<sup>[1,2a,b]</sup>

An all-phosphorus analog of C<sub>5</sub>H<sub>5</sub><sup>−</sup>, the pentaphosphacyclopentadienide or pentaphospholide anion [*cyclo*-P<sub>5</sub>]<sup>−</sup> is a particularly interesting heterocycle.<sup>[3]</sup> Alkali metal salts of [*cyclo*-P<sub>5</sub>]<sup>−</sup> were first synthesized by Baudler and co-workers in 5–12% yield in 1987 by conversion of white phosphorus with sodium or lithium dihydrogen phosphide.<sup>[4]</sup> In contrast to the valence isoelectronic [*cyclo*-N<sub>5</sub>]<sup>−</sup>, that has only been generated as a transient species,<sup>[5]</sup> [*cyclo*-P<sub>5</sub>]<sup>−</sup> is persistent in solution.

The stereoelectronic properties along with the thermodynamic stability of [*cyclo*-P<sub>5</sub>]<sup>−</sup> gave rise to various subsequent synthetic studies. These not only covered metallocene analogs in which [*cyclo*-P<sub>5</sub>]<sup>−</sup> replaces the classical C<sub>5</sub>H<sub>5</sub><sup>−</sup> ligand,<sup>[4b,6]</sup> but also promoted the coordination chemistry of [*cyclo*-P<sub>5</sub>]<sup>−</sup> to a new level, as the additional heteroelements allowed access to supramolecular complexes with multidimensional topology through coordination via the phosphorus lone pairs.<sup>[7]</sup>

However, apart from the coordination chemistry, limited information is still available concerning the reactivity of [*cyclo*-P<sub>5</sub>]<sup>−</sup>. Initial attempts to react M[*cyclo*-P<sub>5</sub>] (M=Li, Na) with alkyl halides resulted in the formation of aggregated polyphosphanes.<sup>[4]</sup> Nevertheless, it was shown that [*cyclo*-P<sub>5</sub>]<sup>−</sup>, stabilized in the coordination sphere of transition metals (Figure 1a, **A**), is reactive towards electrophiles, silylenes as well as elemental iodine (Figure 1a, **B–E**).<sup>[8]</sup>

In 2005 Hey-Hawkins and co-workers showed that Na[*cyclo*-P<sub>5</sub>] (1, Figure 1b) reacts in an unusual way with an ( $\eta^3$ -cyclopropenyl)-Ni complex to give the 1,2-diphospholide anion 1,2-[*cyclo*-(RC)<sub>3</sub>P<sub>2</sub>]<sup>−</sup> (**F**) instead of forming the anticipated 18-electron sandwich complex.<sup>[9]</sup> This example demonstrates that [*cyclo*-P<sub>5</sub>]<sup>−</sup> is a potential source of [P<sub>1–4</sub>]<sup>−</sup> fragments for the construction of heterocyclic systems. Stimulated by our recent results on cycloaddition reactions with aromatic five- and six-membered phosphorus heterocycles, we considered that Na[*cyclo*-P<sub>5</sub>] (1) could act as a precursor for the synthesis of a library of novel phosphorus containing heterocycles (Figure 1).<sup>[10]</sup>

[a] A. Petrov, Dr. N. T. Coles, M. Weber, Prof. Dr. C. Müller  
Institute of Chemistry and Biochemistry  
Freie Universität Berlin  
Fabeckstr. 34/36, 14195 Berlin (Germany)  
E-mail: c.mueller@fu-berlin.de

[b] L. Conrad, Priv.-Doz. Dr. D. Andrae  
Institute of Chemistry and Biochemistry  
Freie Universität Berlin  
Arnimallee 22, 14195 Berlin (Germany)

[c] Dr. N. T. Coles  
School of Chemistry, University of Nottingham  
University Park, Nottingham, NG7 2RD (United Kingdom)

[d] Dr. A. Zagidullin, Dr. V. Miluykov  
Arbuzov Institute of Organic and Physical Chemistry  
FRC Kazan Scientific Center of RAS  
Arbuzov Str. 8, Kazan (Russia)

Supporting information for this article is available on the WWW under <https://doi.org/10.1002/chem.202203056>

© 2022 The Authors. Chemistry - A European Journal published by Wiley-VCH GmbH. This is an open access article under the terms of the Creative Commons Attribution Non-Commercial License, which permits use, distribution and reproduction in any medium, provided the original work is properly cited and is not used for commercial purposes.

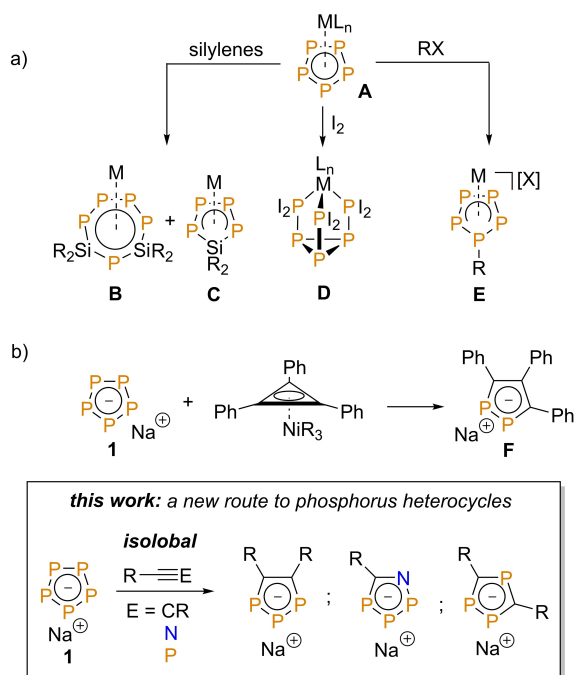
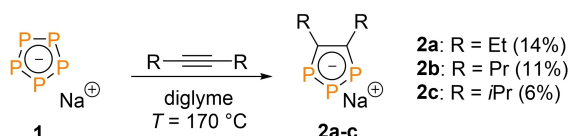


Figure 1. Selected reactions of  $M[\text{cyclo-P}_3]$  and brief summary of this work.

## Results and Discussion

First, we examined the reactivity of  $\text{Na}[\text{cyclo-P}_3]$  (**1**) towards symmetrically substituted aliphatic alkynes as a potential route to hitherto elusive 4,5-dialkyl-1,2,3-triphospholide anions  $1,2,3\text{-}[\text{cyclo}(\text{RC})_2\text{P}_3]^-$  (Scheme 1). The family of these heterocycles is limited to a few species with  $\text{R}=\text{H}$  or  $\text{R}=\text{aryl}$ , which is in clear contrast to the structurally more diverse isomers of the 1,3,4-triphospholide anions  $1,3,4\text{-}[\text{cyclo}(\text{RC})_2\text{P}_3]^-$  ( $\text{R}=\text{alkyl}$ ,  $\text{Me}_3\text{Si}$ ,  $\text{Me}_3\text{SiO}$ ,  $\text{aryl}$ ).<sup>[2b,c]</sup> In fact, aryl derivatives of  $1,2,3\text{-}[\text{cyclo}(\text{RC})_2\text{P}_3]^-$  are accessible through the functionalization of  $\text{K}_3\text{P}_7$  or **1** with aryl-substituted alkynes. However, the attempt to synthesize 4,5-diethyl-1,2,3- $[\text{cyclo}(\text{RC})_2\text{P}_3]^-$  by reacting the electron-rich  $\text{K}_3\text{P}_7$  with hex-3-yne resulted only in a mixture of several unidentified products.<sup>[11]</sup> We thus anticipated that the aromatic  $[\text{cyclo-P}_3]^-$ , that has a delocalized negative charge, might interact with aliphatic alkynes in a desired manner.

Commercially available hex-3-yne, with the sterically accessible triple bond, was used for our initial studies. One equivalent of the alkyne was added to a diglyme solution of **1** and the resulting mixture was stirred under reflux. The synthesis of sodium 4,5-diethyl-1,2,3-triphospholide (**2a**) under these conditions was confirmed by the corresponding  $^{31}\text{P}\{^1\text{H}\}$  NMR



Scheme 1. Synthesis of 4,5-dialkyl-1,2,3-triphospholide anions **2a–c**.

spectrum, which displays two resonances of the  $\text{AB}_2$  spin system at  $\delta(\text{ppm})=241.8$  and  $\delta(\text{ppm})=281.4$  ( $^1J_{\text{P,P}}=473$  Hz; Figure S2 in the Supporting Information). Additionally, the  $^{31}\text{P}\{^1\text{H}\}$  NMR spectrum reveals a set of resonances between  $\delta(\text{ppm})=-50.0$ – $70.0$ , that can be attributed to sodium polyphosphides, which are formed by side reactions involving the decomposition of **1** (Figure S50).<sup>[12]</sup> Interestingly, the Raman spectrum of the insoluble brown precipitate reveals the presence of red phosphorus (Figure S49). Monitoring the course of the reaction by means of NMR spectroscopy further revealed that  $\text{Na}[\text{cyclo-P}_3]$  had been completely consumed after 10–12 h. This time interval was found to be optimal, as **2a** was obtained in a maximum of 14% isolated yield. In order to achieve an even higher conversion of  $\text{Na}[\text{cyclo-P}_3]$ , the stoichiometry between the starting compounds was varied. However, the use of 1.5–2 equiv. of the alkyne only led to an insignificant higher yield. An even larger excess of the nonpolar alkyne provoked the decomposition of  $\text{Na}[\text{cyclo-P}_3]$  in solution and led to a decrease in yield.

The addition of the bulkier oct-4-yne and 2,5-dimethyl-3-hexyne, respectively, to a solution of **1** resulted in the formation of **2b** and **2c**, however, in only low yields (Scheme 1). Moreover, no reaction between **1** and 2,2,5,5-tetramethyl-3-hexyne was observed. Compounds **2a–c** were isolated as very air and moisture sensitive, dark red oils.

The  $^{31}\text{P}$  NMR spectra of **2a** and **2c** (Figures S5 and S10) display two resonances of an  $\text{AA}'\text{BX}_2\text{X}'_2$  and  $\text{AA}'\text{BXX}'$  spin system, respectively. The  $^1\text{H}$  NMR spectra of **2a–c** (Figures S3, S7, and S11) display the chemical shifts of the aliphatic protons between  $\delta(\text{ppm})=1.00$ – $3.00$ . Three signals between  $\delta(\text{ppm})=3.30$ – $3.60$  are attributed to diglyme, which is coordinated to the sodium cation. The 1,2,3- $[\text{cyclo-C}_2\text{P}_3]^-$  carbon nuclei were observed in the  $^{13}\text{C}\{^1\text{H}\}$  NMR spectra (Figures S4, S8, and S12) as multiplet resonances around  $\delta(\text{ppm}) \approx 180$ .

Using DFT methods at the M062X + D3/def2-TZVPD level of theory, we found an energetically feasible bicyclic transition state **TS1** in the reaction between **1** and hex-3-yne, through which **2a** can be formed (Figure 2, for computational details see the Supporting Information).<sup>[13]</sup> This suggests a concerted

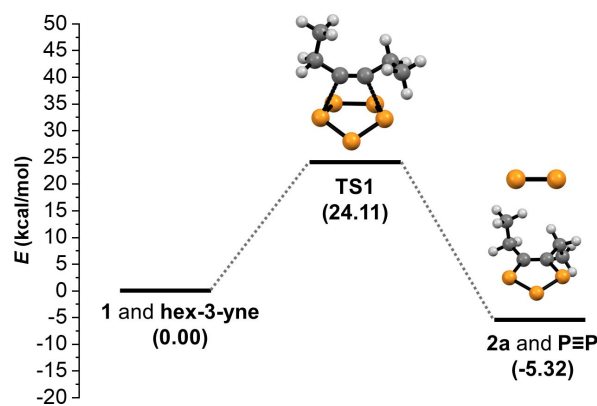
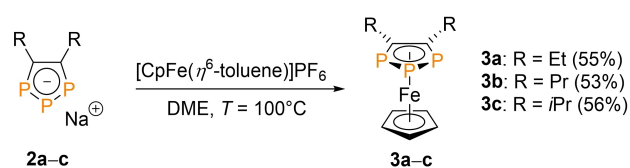


Figure 2. Proposed reaction pathway leading to **2a**. The relative energies of the transition state and the products are given with respect to the starting materials ( $[\text{cyclo-P}_3]^-$  (**1**) and hex-3-yne).

reaction mechanism related to a [4+2] cycloaddition with the elimination of  $[P\equiv P]$ , which reacts further, withdrawing it from the equilibrium, and driving the transformation. The presence of red phosphorus (Figure S49) in the precipitate formed in the reaction between hex-3-yne and **1** can thus be interpreted as the polymerization of highly reactive  $[P\equiv P]$  fragments.<sup>[14]</sup>

Because we were not able to characterize **2a–c** by means of single-crystal X-ray diffraction, we decided to stabilize the anionic heterocycles in the coordination sphere of a metal center. Indeed, we found that **2a–c** easily react with  $[CpFe(\eta^6\text{-Toluene})]PF_6$  in dimethoxyethane (DME) to give the corresponding 4,5-dialkyl-1,2,3-triphosphaferrocenes **3a–c** in approximately 50% yields (Scheme 2). The formation of the sandwich complexes was monitored by means of  $^{31}P\{^1H\}$  NMR spectroscopy, which shows two resonances of the  $AB_2$  spin system between  $\delta(\text{ppm}) = -10.0$ – $60.0$  (Figures S13, S16, and S19). Compounds **3a–c** were isolated as analytically pure solids either by column chromatography or by sublimation.

The cyclic voltammogram of **3a** (Figure S40) at a sweep rate of  $0.1\text{ Vs}^{-1}$  reveals an irreversible oxidation event at a peak potential of  $0.56\text{ V}$  (vs.  $Fc/Fc^+$ ), which is shifted by  $0.2\text{ V}$  anodically compared to 4,5-diphenyl-1,2,3-triphosphaferrocene,<sup>[15]</sup> indicating a stronger  $\pi$ -donor character of **2a**. An irreversible reduction wave at a peak potential of



Scheme 2. Synthesis of 4,5-dialkyl-1,2,3-triphosphaferrocenes **3a–c**.

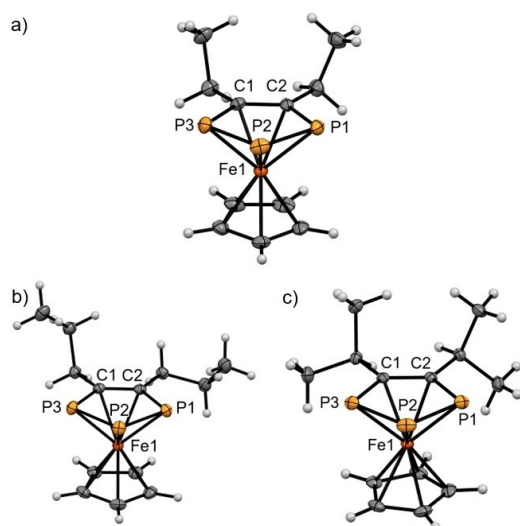


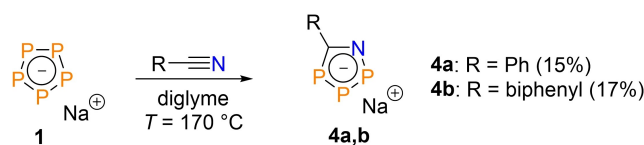
Figure 3. Molecular structures of **3a–c**. Ellipsoids are shown at the 50% probability level. Selected bond lengths [Å] and angles [°]: **3a**: P1–P2: 2.1298(14); C1–C2: 1.412(5); C1–P1: 1.781(3); P1–P2–P3: 99.36(5); P1–C2–C1: 121.0(2). **3b**: P1–P2: 2.1267(6); C1–C2: 1.418(2); C2–P1: 1.7850(16); P1–P2–P3: 99.75(2); P1–C2–C1: 120.61(12). **3c**: P1–P2: 2.1261(4); C1–C2: 1.7885(10); C2–P1: 1.7885(10); P1–P2–P3: 99.560(15); P1–C2–C1: 120.49(7).

$-2.80\text{ V}$  followed by a corresponding anodic signal at  $-0.95\text{ V}$  was registered upon scanning anodically.

Single crystals suitable for single-crystal X-ray diffraction were obtained for all three phosphoferrocenes and the corresponding molecular structures in the crystal are shown in Figure 3. Compounds **3a** and **c** crystallize in the monoclinic space group  $P2_1/n$ , whereas **3b** crystallizes in the monoclinic space group  $P2_1/c$ . The crystallographic characterization confirms the presence of sandwich complexes consisting of one  $\eta^5$ -coordinated 1,2,3-triphospholyl- and one cyclopentadienyl-ring. The derivatives **3a** and **3b** exhibit a perfect eclipsed conformation with the interplanar angles of  $2.82(19)^\circ$  and  $2.95(9)^\circ$ , respectively, while **3c** has a staggered conformation with an interplanar angle of  $21.47(6)^\circ$  in the crystal. The bond lengths and angles in the  $[Cp-Fe-C_2P_3]$  frameworks are similar to the values reported previously for 4,5-diphenyl-1,2,3-triphosphaferrocene.<sup>[15]</sup> The bond lengths P1–P2 and P2–P3 are within the range of  $2.1257(4)$ – $2.1298(14)\text{ Å}$ , which is in between standard P–P single ( $2.20\text{ Å}$ ) and P=P double ( $2.00\text{ Å}$ ) bonds. The P3–C1–C2 and C1–C2–P1 angles are slightly above  $120^\circ$ , whereas P-centered angles are closer to a value of  $100^\circ$ .

Due to the isolobal relationship between the CH fragment and the N-atom, we anticipated a possible reaction between **1** and nitriles under formation of azaphospholide anions. As a matter of fact, azaphospholides of the type  $[cyclo-(RC)_{5-n-x}N_nP_x]^-$  are of fundamental interest as they bridge the gap between the organic cyclopentadienide anion  $C_5H_5^-$  and the fully inorganic aromatic  $[cyclo-N_5]^-$  and  $[cyclo-P_5]^-$ .<sup>[16]</sup> In contrast to phospholides, azaphospholides have proven to be more elusive.<sup>[17]</sup> An important milestone in this field was achieved with the isolation and characterization of the aromatic 1,2-diphosphotriazolide anion  $[cyclo-P_2N_3]^-$ , composed of only phosphorus- and nitrogen-atoms.<sup>[17a]</sup>

We first chose benzonitrile as a substrate, as the electron-withdrawing effect of the phenyl group should promote the desired reaction with  $[cyclo-P_5]^-$  **1**. The substrate (1 equiv.) was added to a solution of **1** and heated to reflux for 12 h (Scheme 3). Interestingly, the  $^{31}P$  NMR spectrum of the crude reaction mixture shows three multiplets of the AMX spin system in the region between  $\delta(\text{ppm}) = 200.0$ – $378.0$  with large coupling constants of  $J = 493$  and  $438\text{ Hz}$  that indicate the presence of P–P bonds. Moreover, the significant downfield shift of one multiplet resonance ( $\delta(\text{ppm}) = 378.0$ ) suggested a P–N bond. Based on the  $^{31}P$  NMR spectrum (Figure S22) we anticipated that the novel P,N-heterocycle 1-aza-2,3,4-triphospholide anion  $1,2,3,4-[cyclo-(RC)NP_3]^-$  (**4a**) had indeed been formed by the formal substitution of a  $[P_2]$  fragment with an RCN moiety in  $[cyclo-P_5]^-$  (Scheme 3).



Scheme 3. Synthesis of 5-aryl-1,2,3,4-azatriphospholide anions **4a** and **b**.

The  $^1\text{H}$  NMR spectrum of **4a** (Figure S23) displays three resonances between  $\delta(\text{ppm})=7.00\text{--}8.26$  of the phenyl group. The noticeable downfield shifted signal at  $\delta(\text{ppm})=8.26$  can be assigned to the protons in *ortho*-position of the phenyl ring. The  $^{13}\text{C}\{^1\text{H}\}$  NMR spectrum of **4a** displays the  $[\text{CNP}_3]^-$  carbon nuclei as a multiplet resonance at  $\delta(\text{ppm})=201.8$  (Figure S24).

We further found that sodium pentaphospholide **1** also reacts with 4-cyanobiphenyl to give **4b**. Compounds **4a** and **4b** were isolated as air and moisture sensitive dark red oils in 15–17% yields. Increasing the reaction time to 24, respectively 48 h, only lead to decomposition of the product. Surprisingly, the reaction of **1** with *m*- and *p*-tolunitrile affords only trace amounts of the desired compounds along with several side products. Moreover, we could neither observe a reaction between **1** and pivalonitrile, nor between **1** and acetonitrile. Instead, after 12 h of reflux, we observed a bleaching of the orange solution along with a precipitation of an insoluble solid.

Because the azatriphospholide anion is a novel compound, we anticipated to perform additional theoretical calculations on the parent 1-aza-2,3,4-triphospholide anion **4**.<sup>[18]</sup> The AIM analysis of **4** reveals five (3;−1) bond critical points (BCPs) and one ring (3;+1) critical point (RCP). The Laplacian of the electron density between all bonds is negative, which is typical for bonds with covalent character (Figure 4, left). The plot of the electron localization function (ELF) also confirms the covalency of the bonds in **4** (Figure 4, right). Additionally, it displays the localization of N and P lone pairs in the ring plane.

The aromaticity of the parent 1-aza-2,3,4-triphospholide anion, which was evaluated by the nucleus independent chemical shift (NICS) method (NICS(0): −15.64), is comparable to  $[\text{cyclo}(\text{CH})_3\text{P}]^-$  (NICS(0): −12.53) and  $[\text{cyclo}(\text{P})_3]^-$  (NICS(0): −16.66).<sup>[19]</sup> Additionally, natural bond orbital (NBO) analysis of the 1-aza-2,3,4-triphospholide anions (Figure 5 and Table S17) reveals an extensive delocalization of  $\pi$ -electrons.<sup>[20]</sup>

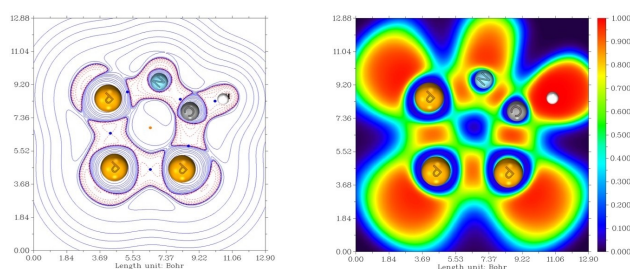


**Figure 4.** Left: Contour plot of the Laplacian of the electron density in **4** (left); BCPs: blue dots; RCP: red dot. Positive contour lines are colored blue; negative contour lines are red. Right: Color-filled map of the electron localization function of **4**.

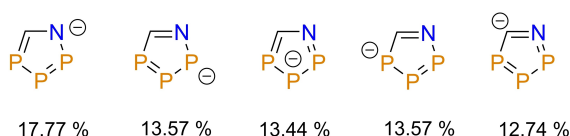


**Figure 5.** Natural resonance theory (NRT) weights of the parent 1-aza-2,3,4-triphospholide anion **4** from an NBO analysis.

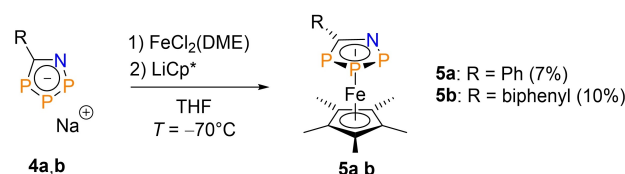
According to the computational data we propose that **4a** could be formed by a similar mechanism as proposed for **2a** (Figure S51). The calculations show the positive reaction energy value for the formation of **4a**. Therefore, we anticipate that the elimination and subsequent polymerization of  $[\text{P}\equiv\text{P}]$  is essential for the reaction to proceed.

As we were again not able to grow crystals of compounds **4a,b**, suitable for crystallographic characterization, we decided to stabilize the corresponding P,N-heterocycles again in the coordination sphere of a metal center. Unfortunately, **4a,b** decompose when reacted with  $[\text{CpFe}(\eta^6\text{-toluene})]\text{PF}_6$  (Scheme 2). Most likely, this is due to the pronounced  $\pi$ -acceptor character of the ligand and the sterically accessible in-plane lone pair of the N-atom (Figure 4, left), which causes a slippage from the  $\eta^5$ - to an  $\eta^1$ -coordination mode with subsequent decomposition of the complex.<sup>[21]</sup> Consequently, we attempted the synthesis of a 1,2,3,4-azatriphosphaferrocene derivative, decorated with the sterically demanding and electron-rich pentamethyl-cyclopentadienyl ( $\text{Cp}^*$ ) ligand. The pure compounds **5a,b** were isolated in 7–10% yields (Scheme 4).

The  $^{31}\text{P}\{^1\text{H}\}$  NMR spectra of **5a** and **b** (Figures S28 and S31) show three multiplets, that form an ABX spin system between  $\delta(\text{ppm})=30.0$  and  $\delta(\text{ppm})=140.0$  ( $^1J_{\text{P,P}}=451$  and  $346$ ;  $^2J_{\text{P,P}}=8$  Hz). The  $^1\text{H}$  and  $^{13}\text{C}\{^1\text{H}\}$  NMR spectra are in line with the proposed structure of **5a,b**, depicted in Scheme 4 (Figures S29, S30, S32 and S33).

The cyclic voltammogram of **5b** (Figure S41) at a sweep rate of  $0.1\text{ V s}^{-1}$  reveals an irreversible oxidation event at a peak potential of  $1.10\text{ V}$  (vs.  $\text{Fc}^*/\text{Fc}^{*+}$ ), followed by an irreversible reduction wave at  $-2.01\text{ V}$  without coupled anodic signals.

Compound **5b** crystalizes in the monoclinic space group  $P2_1/c$  with two enantiomeric molecules in the asymmetric unit and in a ratio of 85(A):15(B) (Figure 6). Here, only the main enantiomer **5b(A)** will be discussed (for the minor enantiomer **5b(B)** see Figure S47 and Tables S10 and S11). The pentamethylcyclopentadienyl and the 1,2,3,4-azatriphospholyl ligands are both  $\eta^5$ -coordinated to the  $\text{Fe}^{\text{II}}$  center with a corresponding  $\text{Cp}^*_{(\text{centroid})}\text{-Fe-CNP}_{3(\text{centroid})}$  angle of  $178.74(10)^\circ$ . The  $\eta^5$ -coordination of the  $[\text{cyclo}(\text{CR})\text{NP}_3]$  ligand confirms the aromatic character of the novel N,P-heterocycle. The interplanar angle between two ligands is  $19.04(13)^\circ$  ( $5.5(4)^\circ$  for **5b(B)**). The P1–P2 bond ( $2.1514(13)\text{ \AA}$ ) is slightly elongated compared to the P2–P3 bond ( $2.1059(14)\text{ \AA}$ ) due to the presence of the highly electronegative nitrogen atom. The P1–N1 bond distance of  $1.702(9)\text{ \AA}$  is similar to the P–N bond distance ( $1.670(1)\text{ \AA}$ ) in the 1,2,3,4-diazadiphospholide anion.<sup>[17d]</sup> The C1–N1–P1 angle of  $119.8(7)^\circ$  is in line with an  $\text{sp}^2$  hybridization of the nitrogen atom.



**Scheme 4.** Synthesis of 5-aryl-1,2,3,4-azatriphosphaferrocenes **5a** and **b**.

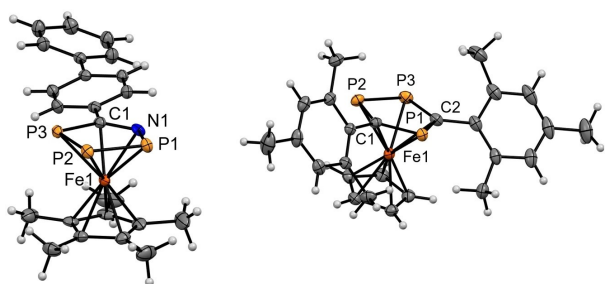


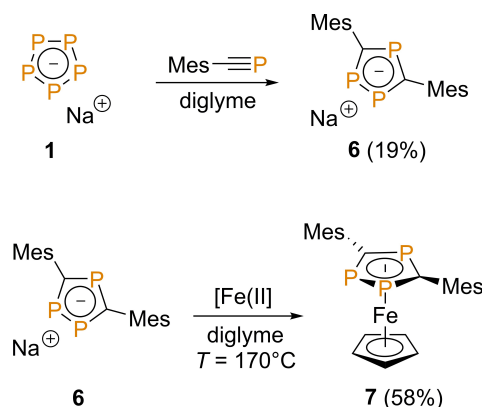
**Figure 6.** Molecular structure of the **5b(A)** (left) and **7** (right) in the crystal. Ellipsoids are shown at the 50% probability level. Selected bond lengths [Å] and angles for **5b(A)** [°]: P1–N1: 1.702(9); P1–P2: 2.1514(13); P3–P2: 2.1059(14); P3–C1: 1.813(2); N1–C1: 1.382(9); P3–P2–P1: 97.37(5); N1–P1–P2: 101.9(4); C1–N1–P1: 119.8(7). For **7**: P2–P3: 2.1296(10); P1–C1: 1.761(2); P1–C1–P2: 121.67(14); C1–P1–C2: 98.91(12); C1–P2–P3: 98.86(9).

Having proven that the pentaphospholide anion reacts with  $C\equiv N$  triple bonds, we consequently attempted the reaction between **1** and phosphalkynes as a potential pathway towards barely explored 1,2,3,4-tetraphospholide anions. In analogy to the use of benzonitrile, preference was given to the use of the kinetically stabilized Mes– $C\equiv P$  (Mes = mesityl).<sup>[22]</sup>

Interestingly, preliminary studies reveal that the sodium 2,5-bismesityl-1,3,4-triphospholide anion **6** was formed in the reaction with 1 equiv. of Mes– $C\equiv P$ , rather than the anticipated 1,2,3,4-tetraphospholide. Apart from the residual resonance of  $[cyclo-P_5]^-$ , the  $^{31}P\{^1H\}$  NMR spectrum of the reaction mixture displays a doublet and triplet at  $\delta(\text{ppm}) = 252.6$  and  $\delta(\text{ppm}) = 263.2$  ( $^2J_{P-P} = 37$  Hz), respectively. Heterocycle **6** was isolated in a maximum yield of 19% (when 2 equiv. of Mes– $C\equiv P$  were used) as a dark red powder. The multinuclear NMR spectroscopic data (Figures S34–S36) match with the previously reported potassium salt of the 2,5-bismesityl-1,3,4-triphospholide anion.<sup>[23]</sup> Taking into account that, in contrast to alkynes and nitriles, the reaction with Mes– $C\equiv P$  proceeds at room temperature and leads to **6**, we anticipate a different reaction mechanism for the formation of the 1,3,4-triphospholide anion. This observation is currently studied separately in more detail. We also found that **1** does not react with Mes\*– $C\equiv P$ , even at elevated temperatures, most likely due to the sterically hindered  $C\equiv P$  triple bond. Much to our delight, we found that **6** also reacts with  $[CpFe(\eta^6\text{-toluene})]PF_6$  in refluxing diglyme to give the sandwich complex **7** in 58% yield (Scheme 5 and Figure 6, see the Supporting Information for full characterization).

## Conclusion

In summary, we have examined the reactivity of  $[cyclo-P_5]^-$  (**1**) towards  $C\equiv E$  ( $E=C, N, P$ ) triple bonds and could demonstrate that **1** acts as a formal source of  $[P_3]^-$  and  $[P_1]^-$  fragments to generate novel, aromatic, five-membered heterocycles. Following the newly developed route starting from  $Na[cyclo-P_5]$ , otherwise elusive 4,5-dialkyl-1,2,3-triphospholides (**2a–c**), 5-aryl-1-aza-2,3,4-triphospholides (**4a** and **b**) as well as sodium 3,5-bismesityl-1,3,4-triphospholide (**6**) are now accessible. DFT



**Scheme 5.** Synthesis of 2,5-bismesityl-1,3,4-triphospholide anion **6** and the corresponding 1,3,4-triphosphaferrocene **7**.

calculations suggest that the formation of **2a** and **4a** occurs via a concerted transition state, in which  $[P\equiv P]$  is substituted by the respective  $[C\equiv E]$  unit ( $E=CR, N$ ), with the simultaneous restoration of the aromatic system. All new compounds react with  $Fe^{II}$  precursors to give the corresponding sandwich complexes of (aza)phosphaferrocenes in moderate to good yields. The formation of the novel 1-aza-2,3,4-triphosphaferrocenes **5a** and **b** serves as an experimental and structural proof of the aromaticity in the corresponding 1-aza-2,3,4-triphospholides **4a** and **b**.

Deposition Numbers 210960 (**3a**), 2150961 (**3b**), 2150963 (**3c**), 2150962 (**5b**) and 2150959 (**7**) contain the supplementary crystallographic data for this paper. These data are provided free of charge by the joint Cambridge Crystallographic Data Centre and Fachinformationszentrum Karlsruhe Access Structures service.

## Acknowledgements

The authors gratefully acknowledge the Freie Universität Berlin for financial support and the High-Performance Computing Service of Zentrale Dateneinrichtung (ZEDAT), Freie Universität Berlin, for computing time. Almaz Zagidullin is grateful for a Russian Science Foundation grant (no. 21-73-10204). Open Access funding enabled and organized by Projekt DEAL.

## Conflict of Interest

The authors declare no conflict of interest.

## Data Availability Statement

The data that support the findings of this study are available in the supplementary material of this article.

**Keywords:** cyclic voltammetry · DFT calculations · heteroferrocenes · phosphorus heterocycles · X-ray diffraction

- [1] a) *Progress in Heterocyclic Chemistry, Vol. 33* (Eds: G. W. Gribble, J. A. Joule), Elsevier, 2021, pp. 1–640; b) K. Ota, R. Kinjo, *Chem. Soc. Rev.* 2021, 50, 10594–10673.
- [2] a) N. T. Coles, A. S. Abels, J. Leidl, R. Wolf, H. Grützmacher, C. Müller, *Coord. Chem. Rev.* 2021, 433, 213729–213756; b) I. A. Bezkishko, A. A. Zagidullin, V. A. Miluykov, O. G. Sinyashin, *Russ. Chem. Rev.* 2014, 83, 555–574; c) D. Heift, Z. Benko, H. Grützmacher, *Chem. Eur. J.* 2014, 20, 11326–11330.
- [3] H. J. Zhai, L. S. Wang, A. E. Kuznetsov, A. I. Boldyrev, *J. Phys. Chem. A* 2002, 106, 5600–5606.
- [4] a) M. Baudler, D. Düster, D. Ouzounis, *Z. Anorg. Allg. Chem.* 1987, 544, 87–94; b) M. Baudler, S. Akpapoglou, D. Ouzounis, F. Wasgestian, B. Meinigke, H. Budzikiewicz, H. Münster, *Angew. Chem. Int. Ed.* 1988, 27, 280–281; *Angew. Chem.* 1988, 100, 288–289.
- [5] C. Zhang, C. Sun, B. Hu, C. Yu, M. Lu, *Science* 2017, 355, 374–376.
- [6] a) M. Baudler, T. Etbach, *Angew. Chem. Int. Ed.* 1991, 30, 580–582; *Angew. Chem.* 1991, 103, 590–592; b) E. Urnèzius, W. W. Brennessel, C. J. Cramer, J. E. Ellis, P. von Ragué Schleyer, *Science* 2002, 295, 832–834.
- [7] J. Bai, A. V. Virovets, M. Scheer, *Science* 2003, 300, 781–783.
- [8] a) C. Riesinger, G. Balázs, M. Bodensteiner, M. Scheer, *Angew. Chem. Int. Ed.* 2020, 59, 23879–23884; *Angew. Chem.* 2020, 132, 24088–24094; b) R. Yadav, T. Simler, S. Reichl, B. Goswami, C. Schoo, R. Köppe, M. Scheer, P. W. Roesky, *J. Am. Chem. Soc.* 2020, 142, 1190–1195; c) H. Brake, E. Peresyphkina, A. V. Virovets, M. Piesch, W. Kremer, L. Zimmermann, C. Klimas, M. Scheer, *Angew. Chem. Int. Ed.* 2020, 59, 16241–16246; *Angew. Chem.* 2020, 132, 16377–16383.
- [9] V. Miluykov, A. Kataev, O. Sinyashin, P. Lönnecke, E. Hey-Hawkins, *Organometallics* 2005, 24, 2233–2236.
- [10] a) L. Dettling, M. Papke, J. A. W. Sklorz, D. Buzsáki, Z. Kelemen, M. Weber, L. Nyulászi, C. Müller, *Chem. Commun.* 2022, 58, 7745–7748; J. Lin, F. Wossidlo, N. T. Coles, M. Weber, S. Steinhauer, T. Böttcher, C. Müller, *Chem. Eur. J.* 2022, 28, e202104135.
- [11] a) I. A. Bezkishko, A. A. Zagidullin, A. V. Petrov, V. A. Miluykov, T. I. Burganov, S. A. Katsyuba, O. G. Sinyashin, *J. Organomet. Chem.* 2017, 844, 1–7; b) R. S. P. Turbervill, A. R. Jupp, P. S. B. McCullough, D. Ergöçmen, J. M. Goicoechea, *Organometallics* 2013, 32, 2234–2244.
- [12] M. Baudler, *Angew. Chem. Int. Ed.* 1987, 26, 419–441; *Angew. Chem.* 1987, 99, 429–451.
- [13] a) Y. Zhao, D. G. Truhlar, *Theor. Chem. Acc.* 2008, 120, 215–241; b) S. Grimme, J. Antony, S. Ehrlich, H. Krieg, *J. Chem. Phys.* 2010, 132, 154104; c) O. Treutler, R. Ahlrichs, *J. Chem. Phys.* 1995, 102, 346.
- [14] G. Rathenau, *Physica* 1937, 4, 503–514.
- [15] A. V. Petrov, A. A. Zagidullin, I. A. Bezkishko, M. N. Khrizanforov, K. V. Kholin, T. P. Gerasimova, K. A. Ivshin, R. P. Shekurov, S. A. Katsyuba, O. N. Kataeva, Y. H. Budnikova, V. A. Miluykov, *Dalton Trans.* 2020, 49, 17252–17262.
- [16] S. Mandal, S. Nandi, A. Anoop, P. K. Chattaraj, *Phys. Chem. Chem. Phys.* 2016, 18, 11738–11745.
- [17] a) A. Velian, C. C. Cummins, *Science* 2015, 348, 1001–1004; b) W. J. Transue, A. Velian, M. Nava, M.-A. Martin-Drumel, C. C. Womack, J. Jiang, G.-L. Hou, X.-B. Wang, M. C. McCarthy, R. W. Field, C. C. Cummins, *J. Am. Chem. Soc.* 2016, 138, 6731–6734; c) C. Pi, Y. Wang, W. Zheng, L. Wan, H. Wu, L. Weng, L. Wu, Q. Li, P. von Ragué Schleyer, *Angew. Chem. Int. Ed.* 2010, 122, 1886–1889; d) C. Charrier, N. Maignot, L. Ricard, P. Le Floch, F. Mathey, *Angew. Chem. Int. Ed.* 1996, 35, 2133–2134; *Angew. Chem.* 1996, 108, 2282–2283.
- [18] T. Lu, F. Chen, *J. Comput. Chem.* 2012, 33, 580–592.
- [19] I. Alkorta, J. Elguero, *Struct. Chem.* 2016, 27, 1531–1542.
- [20] *NBO 7.0*, E. D. Glendening, J. K. Badenhoop, A. E. Reed, J. E. Carpenter, J. A. Bohmann, C. M. Morales, P. Karafiloglou, C. R. Landis, F. Weinhold, Theoretical Chemistry Institute, University of Wisconsin, Madison, 2018.
- [21] G. Frison, F. Mathey, A. Sevin, *J. Phys. Chem. A* 2002, 106, 5653–5659.
- [22] T. Görlich, D. Frost, N. Boback, N. T. Coles, B. Dittrich, P. Müller, W. D. Jones, C. Müller, *J. Am. Chem. Soc.* 2021, 143, 19365–19373.
- [23] C. Heindl, A. Schindler, M. Bodensteiner, E. V. Peresyphkina, A. V. Virovets, M. Scheer, *Phosphorus Sulfur Silicon Relat. Elem.* 2014, 190, 397–403.

Manuscript received: September 30, 2022  
Accepted manuscript online: October 9, 2022  
Version of record online: November 15, 2022